Mass Movement and Preferential Boulder Orientations at the Sandpiper Site on Asteroid Bennu. Y. Tang[1], D.S. Lauretta[1], R.-L. Ballouz[2], D.N. DellaGiustina[1], C.A. Bennett[1], and K.J. Walsh[3], [1]Lunar and Planetary Laboratory, University of Arizona, Tucson, AZ, USA (tangy14@lpl.arizona.edu), [2]Applied Physics Laboratory, Johns Hopkins University, Laurel, MD, USA, [3]Department of Space Studies, Southwest Research Institute, Boulder, CO, USA.

Introduction: NASA's OSIRIS-REx sample return mission investigated near-Earth asteroid (101955) Bennu [1], revealing a boulder-dominated, active surface [2–4] with diverse morphologies [5]. Past missions to asteroids found evidence that seismic shaking and mass movement could be major contributors to surface evolution on small, airless bodies [6,7]. Evidence of mass movement events is globally distributed on Bennu [8]. We previously surveyed a particular area with evidence of mass movement in the northern hemisphere, which we designate Site A; we compared our site survey data with simulations and found possible links between impact-induced seismic shaking and the mass movement [4]. In this study, we conducted similar surveys and simulations for a mass movement site in the southern hemisphere of Bennu, which we designate Site B.

Methodology: Site B is encompassed by one of the OSIRIS-REx mission's candidate sample collection locations, nicknamed Sandpiper, within Bralgah Crater [9] (Fig 1). Sandpiper was observed during the Recon A phase of the mission at image resolutions of 0.014 m/pixel [10]. These high-resolution images enabled survey of boulders at Site B at a smaller size regime than our previous study at Site A (0.2 m vs. 1 m size cut-off) [4]. We used best-fit ellipses to capture the overall shape, size, and orientation of the boulders.

We simulated granular flow under Bennu conditions with the *N*-body code PKDGRAV [11,12], which uses a soft-sphere discrete element method [13] to simulate particle-particle and particle-boundary interactions. This code has been used previously, for example, in analysis of grain motion on Phobos [14] and for simulations of the OSIRIS-REx sample collection event [15,16] and mass movement–inducing seismic shaking [4] on Bennu. Surface objects are simulated as simple single spheres, as well as conglomerations of spheres. Conglomerations allow studies of non-spherical shapes such as ellipsoids, which provide more realistic representations of boulders, including an orientation. This offers better comparisons to survey data and insights into orientational biases, but adds computational complexity and increases run times.

Because the boulder survey for Site B has a size cut-off of 0.2 m diameter, we used a distribution of spheres that ranges from 0.3–0.9 m in diameter, and aggregates with a distribution from 0.3–1.2 m, both following the size frequency distribution of the survey site. The PKDGRAV code provides the locations, orientation, and velocities of boulders throughout the run, allowing detailed analysis of the dynamics of mass movement events.

Similar to previous study, we use the mass flux, Q, to quantify the material transport of mass movements. We define Q as the sum of the mobilized particle masses, m, multiplied by their displacement in the down-slope direction, d_x, normalized by the simulation area and the length of the simulation space in the down-slope direction, l_x.

$$Q = \frac{\sum m * d_x}{(l_x * l_y) * l_x} \quad (1)$$

Seismic shaking in the simulations is achieved by sinusoidal oscillation of a bottom bounding wall. Although real seismic shakings exhibit more complex waveforms, the sinusoidal oscillation allows us to explicitly model and understand the influence of varying the seismic frequency and amplitude in a controlled manner. The frequency of oscillation has been demonstrated to play an important nonlinear factor in the Q of mass movements [4]. Currently, estimates of the seismic properties of kilometer-sized asteroids are not well constrained, and the value of the characteristic frequency, f_{char}, ranges from 0.4 to 0.04 Hz [4,17–20]. Thus, we explore a wide range of frequencies, ranging from 0.08 to 20 Hz, as smaller impacts are more likely to induce higher-frequency shakings [17].

Results: The boulder survey revealed a preferential major-axis orientation bias for boulders in Site B (Fig 2). Using the best-fit ellipses for boulders with ellipticity greater than 0.2, we find a bimodal distribution with peaks at azimuths 95.4° and 163.3° (p-value = 0.822, Fig 2), where 90° is east. We applied the Kolmogorov–Smirnov test (K-S test) to constrain best-fit bimodal modified von Mises distributions. The von Mises distribution is a close approximation to a wrapped normal distribution, allowing a continuous probability distribution on the circle [21]. Because boulder orientations pointing 0° and 180° are the same, we modified the period to be π, allowing opposite angle symmetry.

The global geopotential pattern on Bennu consists of slopes that generally point towards the equatorial region. This environment explains the peak at 95.4° azimuth, which implies that boulders in Site B experienced dominant northward migration, but not the eastward movement implied by the 163.3° azimuth. This process mirrors that inferred for the northern hemisphere Site A, which exhibits southward

migrations with eastern movements. The mechanism for eastern movements inferred for both sites requires further investigations.

Of note is the presence of a large boulder in Site B, which appears to divert materials around it, creating a "wake" in the distribution of mass-movement material (Fig 1). This configuration resulted in an extended region of smoother material just north of the boulder, the area considered for sampling. This morphology provides a unique insight into the effects of movement on boulder orientations, and will be used as comparison to results from our simulations.

Conclusion and Future Work: Survey of boulders at Site B shows possible additional eastern movement of boulders that mirror similar conclusions regarding Site A in the northern hemisphere of Bennu. Simulations of seismic shaking–induced mass movements using Site B characteristics are ongoing. These simulations include a cylindrical structure to simulate the large boulder seen in the survey area and the diverging flow it appears to create.

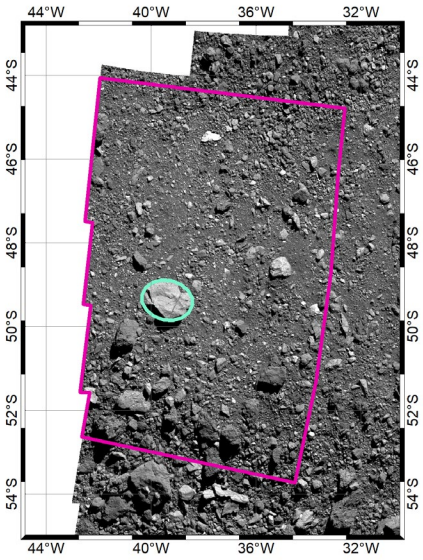

Fig. 1. The survey area of Site B, in the vicinity of the Sandpiper candidate sampling site on Bennu. The general slope is southern high to northern low. The teal ellipse highlights a large boulder that appears to divert the northward material transport.

Fig. 2. (following) A) Rose diagram showing the long-axis orientation of the boulders surveyed in Site B, after averaging the bins with parallel orientations (e.g., 0° vs. 180°). B) Histogram of the long-axis orientation of the boulders surveyed in Site B, with bins of 5°. Bins of parallel orientations are combined. The green line is the best-fit modified bimodal von Mises distribution. C) The empirical distribution function (black line) and cumulative distribution function (green line) of the orientation directions, used for the K-S tests to derive the p-values.

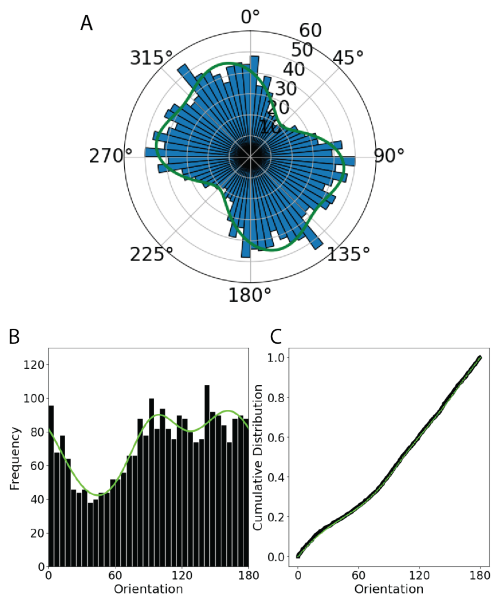

Acknowledgments: This material is based upon work supported by NASA under Contract NNM10AA11C issued through the New Frontiers Program. We are grateful to the entire OSIRIS-REx Team.

References: [1] Lauretta D.S. et al. (2017), *Space Sci Rev, 212*, 925-984. [2] Lauretta D.S. et al. (2019), *Science, 366(6470)*, eaay3544. [3] Jawin E.R. et al. (2022), *Icarus*, *381*, 114992. [4] Tang Y. et al. (2022), *Icarus* (in review). [5] Lauretta D.S. et al. (2019), *Nature, 568*, 55–60. [6] Thomas P.C. et al (2002), *Icarus, 155(1)*, 18-37. [7] Miyamoto H. et al. (2007), *Science, 316(5827)*, 1011-1014. [8] Jawin E.R. et al. (2020), *JGR: Planets, 125*, e2020JE006475. [9] Perry M.E et al. (2022), *Nature Geosciences*, *15*, 447-452. [10] Lauretta D.S. et al. (2021), *Sample Return Missions*, ed. A Longobardo (Elsevier), 163-194. [11] Richardson D.C. et al. (2000), *Icarus, 143*, 45. [12] Zhang Y. et al. (2017), *Icarus, 294*, 98-123. [13] Schwartz S.R. et al. (2012), *Granular Matter, 14*, 363-380. [14] Ballouz R-L. et al. (2019), *Nature Geosciences, 12*, 229-234. [15] Ballouz R-L. et al. (2017), Ph.D. Thesis, UMD [16] Lauretta D.S. et al. (2022), *Science*, *377*(6603), 285–291. [17] Quillen A.C. et al. (2019), *Icarus*, *319*, 312–333. [18] Murdoch N. et al. (2015), *Asteroids IV*, University of Arizona Press. [19] Garcia R.F. et al. (2015), *Icarus*, *253*, 159–168. [20] Goddard J.D. (1990) *Proc R Soc London Ser A: Math Phys Sci*, *430*(1878), 105–131. [21] Peacock, B. et al. (2013). *Statistical distributions*, Wiley.